# Nanoscale electrocrystallisation of Sb and the compound semiconductor AlSb from an ionic liquid

**C. L. Aravinda and W. Freyland***

*Received (in Cambridge, UK) 7th December 2005, Accepted 27th February 2006*
*First published as an Advance Article on the web 10th March 2006*
**DOI: 10.1039/b517243h**

**Aluminium antimonide nanoclusters with an apparent band gap energy of 0.92 ± 0.2 eV have been electrodeposited from the neutral ionic melt $AlCl_3$–1-butyl-3-methylimidazolium chloride {$AlCl_3$–$[C_4mim]^+Cl^-$} at room temperature and have been characterized *in-situ* by electrochemical scanning tunneling microscopy (STM) and spectroscopy (STS).**

The enormous interest in nanoscale materials stems from their fascinating size dependent properties, in particular, specific variation of their catalytic, electronic, or mechanical characteristics. The size, structure and growth patterns and hence their properties can depend on the preparation techniques. Focusing here on electrochemical techniques, room temperature molten salts or ionic liquids (ILs) have proven to be particularly attractive electrolytes for the deposition of various materials. They are characterized by low melting points, very low vapour pressures, high electrolytic conductivities and especially large electrochemical windows of up to 6 V, see *e.g.* ref. 1. It is this last characteristic that enables the electrodeposition of new materials which due to their large deposition potential cannot be deposited from aqueous electrolytes. Recently, ILs have been used successfully to deposit a variety of nanostructured materials such as functionalized nanoporous gold,[2] $C_{60}$ fullerene thin films,[3] elemental semiconductors,[4] nanocrystalline metals and alloys by electrochemical means.[5] The research in this direction is motivated by the prospect to control the various deposition parameters precisely and to design the strategy for deposition of metal, alloy and semiconductor nanostructures by employing *in-situ* nanoscale probe techniques. The group III–V compound semiconductors in general and Sb based semiconductors in particular are finding increasing importance for use as barrier materials in high speed electronics and long-wavelength optoelectronic devices.[6,7] Here we present the first report on nanoscale electrodeposition of the compound semiconductor $Al_xSb_y$ from an {$AlCl_3$–$[C_4mim]^+Cl^-$} melt by *in-situ* characterization with electrochemical STM and STS. The bulk Al–Sb alloy phase diagram is characterized by a stoichiometric compound AlSb which melts congruently at 1058 °C.

$[C_4mim]^+Cl^-$ was synthesized as described earlier.[8] Anhydrous $AlCl_3$ (Fluka, >99%) was sublimed twice under vacuum and the resulting white crystals were used for the melt preparation. A neutral {$AlCl_3$–$[C_4mim]^+Cl^-$} melt was obtained by mixing equal moles of $AlCl_3$ crystals and $[C_4mim]^+Cl^-$. A highly viscous $SbCl_3$–$[C_4mim]^+Cl^-$ melt was formed by mixing $SbCl_3$ (Alfa, >99.99%) with $[C_4mim]^+Cl^-$ in a molar ratio of 45 : 55.[9] A melt containing Sb(III) with an effective concentration of ~1 mM was prepared by adding an appropriate amount of the $SbCl_3$–$[C_4mim]^+Cl^-$ melt to the {$AlCl_3$–$[C_4mim]^+Cl^-$ melt and stirring for 24 h. All the above processes were carried out under high purity argon atmosphere at a temperature of 294 K.

An overview of the redox processes during Sb electrodeposition from an {$AlCl_3$–$[C_4mim]^+Cl^-$} ionic liquid is obtained by cyclic voltammetric studies. Fig. 1 shows the voltammograms on Au(111) recorded at different sweep rates in the melt containing ~1 mM Sb(III). The redox couple C1/A1 around 730 mV corresponding to a two electron oxidation process of Sb(III) to Sb(V) is observed in agreement with earlier studies in a similar melt.[10] In the present neutral melt Al(III) mainly exists as $AlCl_4^-$ and is not reducible in the potential range of Sb deposition and hence excludes the deposition of Al. $SbCl_3$ due to the equilibrium reaction with $AlCl_4^-$ forms $SbCl_4^-$ and $SbCl_2^+$ complex ions.[11] The reduction waves indicated in the range from C2 to C3 we attribute to the underpotential deposition (UPD) of Sb, see below. The reduction peak C4 exhibits a clear asymmetric wing towards cathodic potential which can be explained by Al codeposition, see the STM results below. The broad hump C5 is due to AlSb deposition. The strong anodic peak around 290 mV (A2) encompasses several oxidation processes including Sb and $Al_xSb_y$ stripping. With increasing Sb(III) concentration in the melt, this peak splits into two anodic peaks A2 and A3 at 10 mV and 440 mV, respectively, as shown in the inset of the Fig. 1.

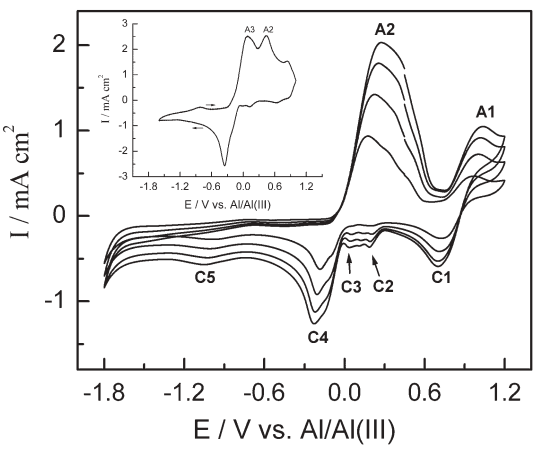


**Fig. 1** Cyclic voltammograms of {$AlCl_3$–$[C_4mim]^+Cl^-$} (1 : 1) ionic melt containing ~1 mM Sb(III) on Au(111) at sweep rates of 20, 40, 60 and 80 mV $s^{-1}$. Inset shows the cyclic voltammogram recorded in melt containing ~5 mM Sb(III) at a sweep rate of 100 mV $s^{-1}$. Temperature 294 K.

*Institute of Physical Chemistry, University of Karlsruhe (TH), Kaiserstrasse 12, D-76128, Karlsruhe, Germany. E-mail: Werner.Freyland@chem-bio.uni-karlsruhe.de; Fax: +49-721-608-6662; Tel: +49-721-608-2100*

*In-situ* STM experiments were performed in feedback control mode with a Molecular Imaging Picoscan® STM controller under potentiostatic conditions with a specially designed in house built electrochemical STM setup as described in ref. 12. A fresh 200–300 nm thick gold film evaporated onto a chromium covered quartz plate (12 × 12 $mm^2$, Berliner Glas KG, Germany) was annealed in a $H_2$ flame and cooled slowly in a $N_2$ stream prior to use as a working electrode. A pre-cleaned Teflon electrochemical cell (effective area of 0.36 $cm^2$) was sealed on to the gold substrate using a Teflon coated O-ring. An Al ring and Al wire (>99.99%, Alfa Acer, Germany) dipped into the melt served as the counter and reference electrodes, respectively. The STM tip was freshly prepared by etching tungsten wire (0.25 mm diameter, >99.98%, Alfa) in a NaOH solution (2 mol $l^{-1}$). To avoid the effect of faradaic currents, the tips were coated *via* electrophoresis with an epoxide electropaint (BASF ZQ 84-3225 0201, Germany) and cured at 150 °C for 2 h and subsequently at 200 °C for 10 min. The whole setup for the EC-STM studies was assembled in an argon filled glovebox ($O_2$ and $H_2O$ < 1 ppm) and mounted in a clean and Ar-filled airtight stainless steel container to prevent contamination and to ensure relatively long measurement times.

To get an insight into the electrodeposition process here we focus on the results of the STM experiments performed in two different potential regions: first, the UPD and overpotential deposition (OPD) region of Sb and, secondly, the deposition of $Al_xSb_y$ nanoclusters. In the potential range positive of the redox couple C1/A1, terrace structures of flame annealed Au(111) were seen. Upon changing the potential into the UPD range, 6–16 nm wide and up to ~45 nm long Sb 2D nanostripes appear all over the substrate surface (Fig. 2a). The height of the nanostripes is 2.7 ± 0.2 Å (see height profile). This value is expected for a monolayer of Sb. An atomically resolved STM image of the 2D stripes reveals a highly ordered structure of the Sb $\sqrt{7} \times \sqrt{7}$ superlattice having quasi-hexagonal symmetry with interatomic distances of 7.6 ± 0.2 Å and 7.8 ± 0.2 Å (Fig. 2b). A similar superlattice structure has been observed by Ward and Stickney by LEED studies of the deposition of Sb on Cu(111).[13] After about 30 min the 2D nanostripes merge with one another and a two dimensional worm like network structure evolves (STM picture not shown) and subsequently develops into an almost complete monolayer. Reducing the potential further below 0 V a large number of small monoatomically high islands occurs (Fig. 2c) which exhibit similar facets and identical symmetry (Fig 2d) as that of the 2D nanostripes. The islands coalesce to form deposit domains and begin to grow three dimensionally by the Stransky–Krastanov growth mode when further deposition was promoted at decreasing potentials. When the substrate potential was extended well below −500 mV, drastic changes in the STM pictures were seen. Three dimensional clusters of $Al_xSb_y$ appear. At a substrate potential of −1000 mV the clusters continue to grow in 3D with time to form narrowly size dispersed clusters exhibiting a height of ~6 nm and a width of ~50 nm (see height profile in Fig. 3).

$Al_xSb_y$ clusters were characterized by *in-situ I–U* spectroscopy positioning the tip just above the cluster of interest (see *e.g.* the tip position in Fig. 3a). The STS curves were measured at different sites and clusters and were recorded rapidly (~200 μs) at a set point current of 20 nA. Since the tip bias voltage was scanned in a wide range from −1.2 to 1.2 V during the acquisition of *I–U* curves, the quality of the tip coating was carefully monitored before and after the spectra acquisition which showed Faraday currents of <20 pA. For comparison, spectra of the bare gold

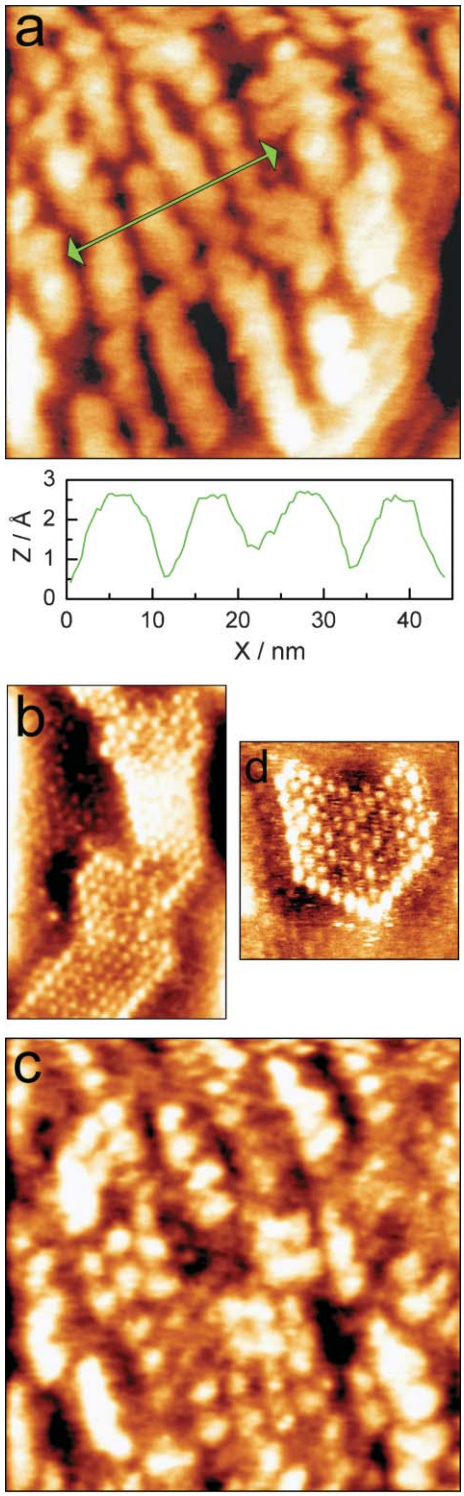


**Fig. 2** (a) STM image (100 × 100 $nm^2$) showing the UPD of Sb 2D nanostripes at 100 mV on Au(111) and the height profile (see double headed arrow), (b) 13 nm × 20 nm high resolution STM image of a Sb nanostripe with $\sqrt{7} \times \sqrt{7}$ super lattice, (c) STM image (100 × 100 $nm^2$) showing the OPD of Sb at −250 mV and (d) 11 × 11 $nm^2$ high resolution STM image of a Sb island deposited on UPD Sb monolayer. $E_{tip}$ = −50 mV, $I_{tunn}$ = 1 nA.

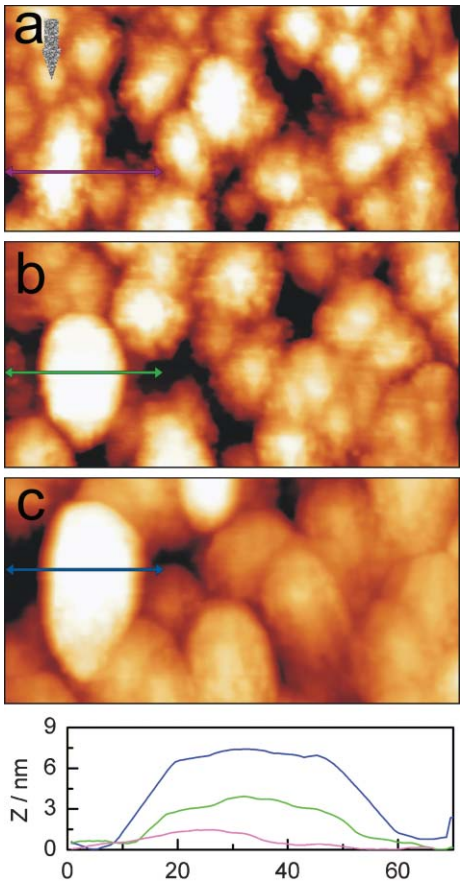


**Fig. 3** Representative *in-situ* STM pictures (200 × 100 nm$^2$) showing the 3D growth of $Al_xSb_y$ nanoclusters with time: (a) after 3 min, (b) after 8 min and (c) after 20 min. $E = -1$ V, $E_{tip} = -0.7$ V, $I_{tunn} = 1$ nA; and the height profiles for the nanocluster.

surface were also recorded prior to the deposition which show typical metallic behavior (see inset Fig. 4). A tunneling spectrum obtained for an $Al_xSb_y$ cluster of ~20 nm in size is shown in Fig. 4. From the spectrum it is apparent that the cluster exhibits semiconductor behavior. The band gap is found to be 0.92 ± 0.2 eV which is clearly smaller than the bulk value for the indirect-gap semiconductor AlSb, *i.e.* ~1.6 eV.[14] The difference between these values may be due to a size effect of the cluster studied and in addition, deviations from stoichiometry which result in a relatively high doping of the cluster. Interestingly, with increasing size of the cluster the energy gap is also found to increase. A detailed study of the dependence of the energy gap on the cluster size and the melt composition is under way and will be published in the future.

Hitherto most of the methods reported to fabricate compound semiconductor nanostructures are based on molecular beam or sputtering techniques under UHV conditions. The present EC-STM study shows the viability of electrochemical methods to deposit less noble compound semiconductors such as AlSb on the

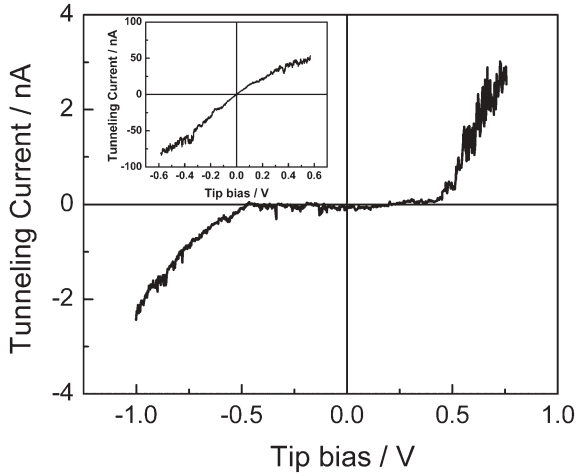


**Fig. 4** A typical *I–U* tunneling spectrum for $Al_xSb_y$ cluster (for tip position see Fig. 3a). Inset shows *I–U* tunneling spectrum for the bare Au (111) substrate. $I_{tunn}$ = 20 nA.

nanometer scale from an ionic liquid. The method also looks very promising to deposit various Sb based compound semiconductor nanostructures containing two or more elements such as InSb, GaSb, AlInSb and GaInAlSb. The 2D layer of Sb deposited in this study was found to be quite stable even at open circuit potential. Since the UPD of Al can also be achieved just by changing the acidity of the melt,[5] there is a possibility to deposit epitaxial Al–Sb compound semiconductor layers by electrochemical atomic layer epitaxy.[15]

Financial support of this work by the DFG Center of Functional Nanostructures, University of Karlsruhe, is acknowledged.

## Notes and references

1 *Ionic Liquids in Synthesis*, ed. P. Wasserscheid and T Welton, Wiley-VCH, Weinheim, 2003.
2 J. F. Huang and I. W. Sun, *Adv. Funct. Mater.*, 2005, **15**, 989.
3 D. Deutsch, J. Tarábek, M. Krause, P. Janda and L. Dunsch, *Carbon*, 2004, **42**, 1137.
4 I. Mukhopadhyay and W. Freyland, *Chem. Phys. Lett.*, 2003, **377**, 223.
5 C. L. Aravinda and W. Freyland, *Chem. Commun.*, 2004, 2754; C. L. Aravinda, I. Mukhopadhyay and W. Freyland, *Phys. Chem. Chem. Phys.*, 2004, **6**, 5225.
6 M. Razeghi, *Eur. Phys. J.: Appl. Phys.*, 2003, **23**, 149.
7 H. Baaziz, Z. Charifi and N. Bouarissa, *Mater. Chem. Phys.*, 2001, **68**, 197.
8 F. Endres and W. Freyland, *J. Phys. Chem. B*, 1998, **102**, 10229.
9 K. Carpenter and M. W. Verbrugge, *J. Mater. Res.*, 1994, **9**, 2584.
10 M. H. Yang and I. W. Sun, *J. Appl. Electrochem.*, 2003, **33**, 1077.
11 M. Lipsztajn and R. A. Osteryoung, *Inorg. Chem.*, 1985, **24**, 3492.
12 A. Shkurankov, F. Endres and W. Freyland, *Rev. Sci. Instrum.*, 2002, **73**, 102.
13 C. Ward and J. L. Stickney, *Phys. Chem. Chem. Phys.*, 2001, **3**, 3364.
14 S. M. Sze, *Physics of Semiconductor Device*, 2nd edn, Wiley Interscience, New York, 1981, pp. 848–849.
15 J. L. Stickney, in *Electroanalytical chemistry A Series of Advances*, ed. A. J. Bard and I. Rubinstein, Marcel Dekker, New York, 1999, p. 75.